

State population transfers using Rabi oscillations

Mahadevan Subramanian* and Drishti Baruah†
Department of Physics
Indian Institute of Technology Bombay

Guides: Barak Dayan and Jeremy Raskop
AMOS and Department of Chemical Physics,
Weizmann Institute of Science, Rehovot, Israel
(Dated: July 30, 2021)

In this report, we explore methods to complete state transfer in Rubidium 87 5S and 5P levels. The methods employed for the same is STIRAP and we specifically look into a case of very unequal peaks for the pulses while also simulating examples of N -STIRAP and cavity-STIRAP. We successfully simulated an adiabatic state population transfer with an efficiency of 99.5% with coherent Rabi pulses of Blackman shape with peaks of 100 MHz and 10 MHz with single photon detuning of 1 GHz and two photon detuning of 2.18 MHz over a $25\mu\text{s}$ timescale.

CONTENTS

Introduction	1
I. Rabi Oscillations	1
A. Jaynes-Cummings Hamiltonian	1
B. The Maxwell-Bloch equations	2
C. Collapse and revival of Atomic Oscillations	2
II. Rabi Oscillations in Rubidium-87	3
A. Hyperfine structure of ^{87}Rb	3
B. Rabi Oscillations for the hyperfine splitting	4
C. Rabi oscillations in the D_2 line	5
III. Stimulated Raman Adiabatic Passage	5
A. Theory	5
B. Importance of two photon detuning	7
C. Robustness of the process	7
D. N -STIRAP	8
E. Cavity STIRAP	9
F. Simulations	9
IV. Conclusion and discussion	10
Acknowledgements	10
Code availability	11
References	11

INTRODUCTION

The problem of an atom interacting with an electromagnetic had received semi-classical treatments which had however failed to explain all the characteristics of such a system. It received a proper quantum treatment

where the field was quantized in the Jaynes-Cummings Hamiltonian [1]. This successfully explained very important characteristics of the system like Rabi oscillations [2] and the collapse and revival of the system [3, 4]. Currently Rabi oscillations are extensively used for quantum information processing [5]

In section I we explore the nature of these Rabi oscillations and their signature behavior. In section II we explore the theory behind driving Rabi oscillations in Rubidium-87 and reach two constants which are proportionality constants for the Rabi oscillations we wish to drive given by $\mathcal{K}_{1,2}$ and $\mathcal{K}_{2,3}$. In section III, along with some STIRAP theory we present simulations for state population transfer from $|F=1, m=1\rangle$ to $|F=3, m=3\rangle$ using $|F=2, m=2\rangle$ as an intermediate state in the ladder STIRAP.

I. RABI OSCILLATIONS

A. Jaynes-Cummings Hamiltonian

A two-state atom, with two energy eigenvalues, is described by a state space spanned by the two energy eigenstates $|e\rangle$ and $|g\rangle$. An arbitrary state vector $|\psi(t)\rangle$ can be expressed as a superposition of the two orthogonal states:

$$|\psi(t)\rangle = c_g |g\rangle + c_e |e\rangle \quad (1)$$

The Hamiltonian operator of the two-level atom in the energy representation is

$$\mathbf{H}_A = E_e |e\rangle\langle e| + E_g |g\rangle\langle g| \quad (2)$$

Setting the zero of energy to the ground state energy of the atom simplifies this to $\mathbf{H}_A = E_e |e\rangle\langle e| = \hbar\omega_{eg} |e\rangle\langle e|$ where ω_{eg} is the resonance frequency of transitions between the sub-levels of the atom.

$$\mathbf{H}_F = \hbar\omega_c \left(\hat{a}_c^\dagger \hat{a}_c + \frac{1}{2} \right) \quad (3)$$

* mahadevan_s@iitb.ac.in

† 190260019@iitb.ac.in

\mathbf{H}_F is the Hamiltonian of the quantized electromagnetic field where we are only considering the resonant mode of the cavity.

Now we obtain the dipole atom-field interaction Hamiltonian, given by, $\mathbf{H}_{A-F} = -\vec{\mathbf{d}} \cdot \vec{\mathbf{E}}(\vec{x}_A, t)$.

The dipole moment operator is represented by

$$\vec{\mathbf{d}} = -(\sigma^- \vec{M}^* - \sigma^+ \vec{M}) \quad (4)$$

where the dipole matrix element $\vec{M} = \epsilon_0 \langle g | \vec{x} | e \rangle$. We assume that the electric field is due to a monochromatic electromagnetic wave (as per the Jaynes Cummings model). So the electric field of the single mode is given by $\vec{E} = \sqrt{\frac{2\pi\hbar\omega_c}{V}} \vec{u}_c (\hat{a}_c - \hat{a}_c^\dagger)$. We define

$\hbar g_c = i\sqrt{\frac{2\pi\hbar\omega_c}{V}} \langle e | \vec{d} | g \rangle \cdot \vec{u}_c$. Thus we get

$$\mathbf{H}_{AF} = \hbar[(g_c \hat{\sigma}_+ \hat{a}_c - g_c^* \hat{\sigma}_- \hat{a}_c^\dagger) + (g_c^* \hat{\sigma}_- \hat{a}_c - g_c \hat{\sigma}_+ \hat{a}_c^\dagger)] \quad (5)$$

where $\hat{\sigma}_+ = |e\rangle\langle g|$, $\hat{\sigma}_- = |g\rangle\langle e|$ and $\hat{\sigma}_- = |g\rangle\langle e|$ are the raising and lowering operators.

We go into the Hamiltonian picture to study the time dependence and get: ($\mathbf{H}_0 = \mathbf{H}_A + \mathbf{H}_F$)

$$\begin{aligned} \mathbf{H}_{AF}(t) &= e^{i\hat{H}_0 t/\hbar} \mathbf{H}_{AF} e^{-i\hat{H}_0 t/\hbar} \\ &= \hbar(g_c \hat{\sigma}_+ \hat{a}_c^\dagger e^{i(\omega_c + \omega_{eg})t} + g_c^* \hat{\sigma}_- \hat{a}_c e^{-i(\omega_c + \omega_{eg})t} \\ &\quad - g_c^* \hat{\sigma}_- \hat{a}_c^\dagger e^{-i(\omega_{eg} - \omega_c)t} - g_c \hat{\sigma}_+ \hat{a}_c e^{i(\omega_{eg} - \omega_c)t}) \end{aligned} \quad (6)$$

Now we make the **Rotating Wave approximation** $|\omega_{eg} - \omega_c| \ll \omega_{eg} + \omega_c$ which holds due to resonance and we can ignore the anti-resonant terms altogether. So we get

$$\mathbf{H}_{AF}(t) = -\hbar(g_c^* \hat{\sigma}_- \hat{a}_c^\dagger e^{-i(\omega_{eg} - \omega_c)t} + g_c \hat{\sigma}_+ \hat{a}_c e^{i(\omega_{eg} - \omega_c)t}) \quad (7)$$

$\delta = \omega_{eg} - \omega_c$ is called the detuning between field and atomic resonance.

We finally go back to the Schrodinger's picture and get

$$\begin{aligned} \mathbf{H}_{AF} &= e^{-i\hat{H}_0 t/\hbar} \mathbf{H}_{AF}(t) e^{i\hat{H}_0 t/\hbar} \\ &= \hbar g_c (\hat{\sigma}_+ \hat{a}_c + \hat{\sigma}_- \hat{a}_c^\dagger) \end{aligned} \quad (8)$$

So the full Jaynes-Cummings Hamiltonian is given as follows: (ignoring the constant term $1/2\hbar\omega_c$, which represents the zero-point energy)

$$\begin{aligned} \mathbf{H}_{JC} &= \mathbf{H}_A + \mathbf{H}_F + \mathbf{H}_{A-F} \\ &= \hbar\omega_c \hat{a}_c^\dagger \hat{a}_c + \hbar\omega_{eg} |e\rangle\langle e| + \hbar g_c (\hat{\sigma}_+ \hat{a}_c + \hat{\sigma}_- \hat{a}_c^\dagger) \end{aligned} \quad (9)$$

B. The Maxwell-Bloch equations

We can describe our two-level system using a density matrix

$$\rho = \begin{bmatrix} \rho_{ee} & \rho_{eg} \\ \rho_{ge} & \rho_{gg} \end{bmatrix}$$

Then the time evolution of the components of this matrix is described using the following equations: (Here δ is the detuning, γ is the decay constant of the atom, κ is the cavity dissipation rate, $\bar{\rho}_{ge} \equiv \rho_{ge} e^{-i\delta t}$ and $\bar{\rho}_{eg} \equiv \rho_{eg} e^{i\delta t}$).

$$\frac{d\rho_{gg}}{dt} = \gamma\rho_{ee} + \frac{i}{2}(\Omega^* \bar{\rho}_{eg} - \Omega \bar{\rho}_{ge}) \quad (10)$$

$$\frac{d\rho_{ee}}{dt} = -\gamma\rho_{ee} + \frac{i}{2}(\Omega \bar{\rho}_{ge} - \Omega^* \bar{\rho}_{eg}) \quad (11)$$

$$\frac{d\bar{\rho}_{ge}}{dt} = -\left(\frac{\gamma}{2} + i\delta\right) \bar{\rho}_{ge} + \frac{i}{2}\Omega^*(\rho_{ee} - \rho_{gg}) \quad (12)$$

$$\frac{d\bar{\rho}_{eg}}{dt} = -\left(\frac{\gamma}{2} - i\delta\right) \bar{\rho}_{eg} + \frac{i}{2}\Omega(\rho_{gg} - \rho_{ee}) \quad (13)$$

Upon analysing the population of the two atomic states as a function of time, we observe an oscillation in the population difference. This oscillation is called the **Rabi-oscillation**. It occurs with a frequency called the Rabi frequency, defined as $\Omega = d_{g,e} \cdot \vec{E}_0/\hbar$.

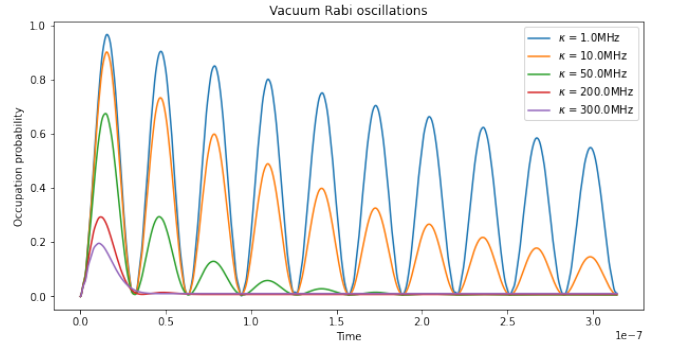


FIG. 1. Shown above is a simulation of a two level atom which has been entangled with a cavity with 16 fock states which starts off in the first excited state. QuTip [6, 7] has been used for the simulation. The value of the coupling $g = 100$ MHz, the decay for the atom is $\gamma = 3$ MHz and the cavity decay is κ which is varying.

C. Collapse and revival of Atomic Oscillations

The interaction Hamiltonian can only cause transitions of the type $|e\rangle |n\rangle \leftrightarrow |g\rangle |n+1\rangle$, where these product states are referred to be as the bare states of the Jaynes-Cummings model. For a fixed n , the dynamics of the system are confined to the two dimensional space of product states $\{|e\rangle |n\rangle, |g\rangle |n+1\rangle\}$.

The Jaynes-Cummings Hamiltonian can be written as:

$$\hat{H}_{JC} = \begin{bmatrix} n\hbar\omega_c + 1/2\hbar\omega_0 & \hbar\Omega\sqrt{n+1} \\ \hbar\Omega\sqrt{n+1} & (n+1)\hbar\omega_c - 1/2\hbar\omega_0 \end{bmatrix} \quad (14)$$

where the eigenvalues are

$$E_{\pm} = (n + \frac{1}{2})\hbar\omega_0 \pm \hbar\sqrt{(\omega_0 - \omega_k)^2 + 4\Omega^2(n+1)} \quad (15)$$

On resonance, we get

$$E_{\pm} = \left(n + \frac{1}{2}\right)\hbar\omega_0 \pm g_0\hbar\sqrt{n+1} \quad (16)$$

where $g_0 = 2\Omega$. Upon further calculations[4], we find that the expression for the population inversion of atomic levels is given by We realise upon plotting this that collapse and revival occurs in case of interaction of a two-level atom with a cavity prepared in a coherent way.

$$W(t) = e^{-N} \sum_{n=0}^{\infty} \frac{N^n}{\sqrt{n!}} \cos 2\Omega_r \sqrt{n+1} t \quad (17)$$

It has been shown [3] that the Rabi oscillations decay at an early stage of the atom–field interaction and reappear at a later stage, but with a smaller amplitude. The following plot shows the occurrence of collapse and revival upon plotting the occupation probability of population in the excited state with respect to time.

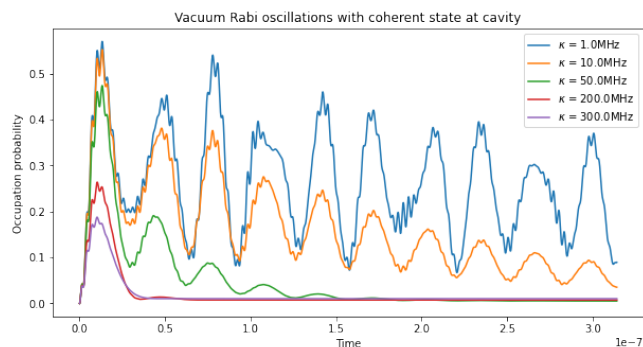


FIG. 2. Shown above is a simulation of a two level atom which has been entangled with a cavity with 16 fock states which starts off in the coherent state with $\alpha = 1$. The value of the coupling $g = 100$ MHz, the decay for the atom is $\gamma = 3$ MHz and the cavity decay is κ which is varying.

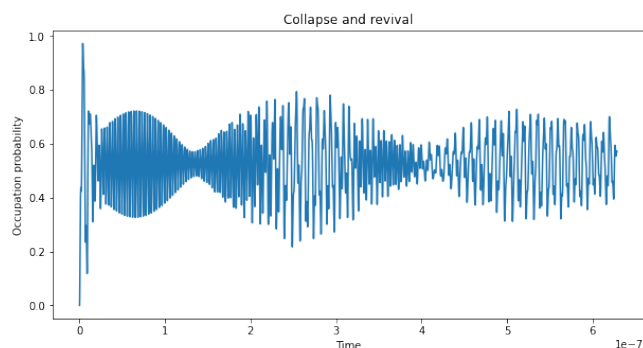


FIG. 3. Demonstration of collapse and revival for a cavity with 32 fock states which starts off in the coherent state of $\alpha = 4$. As we can see the probability dies down and goes to 0.5 a little after $0.1\mu\text{s}$ and then again rises and oscillates.

II. RABI OSCILLATIONS IN RUBIDIUM-87

Rubidium-87 is one of the two naturally occurring isotopes of Rubidium other than ^{85}Rb . Due to its energy level structure and certain characteristics, it is quite a popular atom for quantum and atom optics experiments. We will first discuss the hyperfine structure of ^{87}Rb .

A. Hyperfine structure of ^{87}Rb

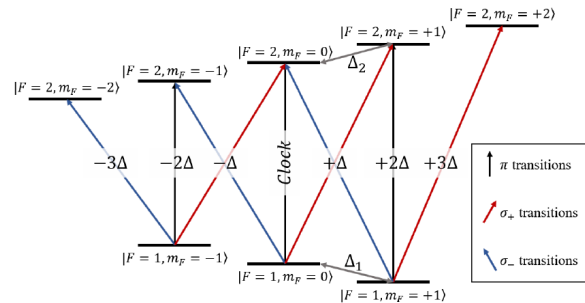


FIG. 4. Hyperfine splitting of levels in Rubidium-87. Image taken from [8]

The ground state of ^{87}Rb which is the $5^2\text{S}_{1/2}$ undergoes a splitting as can be seen figure 4. The notation for the state follows as $n^{2S+1}\text{L}_J$. There are two hyperfine levels formed due to the coupling between the total electron angular momentum ($\mathbf{J} = \mathbf{L} + \mathbf{S}$) and the nuclear angular momentum (\mathbf{I}) and so we write the total angular momentum as $\mathbf{F} = \mathbf{J} + \mathbf{I}$. Here \mathbf{L} and \mathbf{S} are the orbital angular momentum and for the electronic ground state we would have $J = 1/2$ since $L = 0$, $S = 1/2$ and nuclear spin is $I = 3/2$ [9], Now for the addition of angular momentum we have F range between $|J - I|$ and $J + I$ in integer steps. Hence for the state with $L = 0$ we only can have $F = 1, 2$ with each hyperfine level split into $2F + 1$ magnetic sub-levels.

Using the dipole moment spherical tensor as that for defining state transfer we can see using the Wigner-Eckhart Theorem [10] that we would require $\Delta F = 0, \pm 1$ and Δm_F . The $\Delta F = 0$ transitions occur in radio frequency ($10^4 - 10^5$ Hz) and $\Delta F = \pm 1$ are in the microwave region and is about 6.8 GHz [8]. The hyperfine Hamiltonian which describes the coupling between \mathbf{J} and \mathbf{I} has the following form [11].

$$H_{hfs} = \left(A_{hfs} + \frac{3B_{hfs}}{4I(2I-1)J(2J-1)} \right) \mathbf{I} \cdot \mathbf{J} + B_{hfs} \frac{3(\mathbf{I} \cdot \mathbf{J})^2 - I(I+1)J(J+1)}{2I(2I-1)J(2J-1)} \quad (18)$$

We define $K = F(F+1) - I(I+1) - J(J+1)$. The $L = 0 \rightarrow L = 1$ transition is referred to as the D

line and due to the coupling is split into two components, the D₁ line ($5^2S_{1/2} \rightarrow 5^2P_{1/2}$) and the D₂ line ($5^2S_{1/2} \rightarrow 5^2P_{3/2}$) and equation 18 shows the hyperfine Hamiltonian for both these transitions.

Here A_{hfs} is the magnetic dipole constant and B_{hfs} is the electric quadrupole constant. We can see that the B_{hfs} term is only of concern for the D₂ transition when $J \neq 1/2$ and so for now is not of any concern to us since we are interested in the microwave transition.

The value $A_{hfs} = \hbar 3.41734130545215(5)$ GHz is also referred to as the hyperfine structure constant [12]. The eigen energies for H_{hfs} can be seen to be $A_{hfs}K/2$ and corresponds to $-1.25A_{hfs}$ and $0.75A_{hfs}$ for $F = 1$ and $F = 2$ respectively. The total splitting hence is $2A_{hfs} = \hbar 6.8346826109043(1)$ GHz.

B. Rabi Oscillations for the hyperfine splitting

In the presence of a static magnetic field the Hamiltonian of the atom is the following

$$H_B = \mu_B \mathbf{B} \cdot (g_S \mathbf{S} + g_I \mathbf{I}) \quad (19)$$

Here the $g_S = 2.0023193043737(80)$ and $g_I = -0.0009951414(10)$ which are the Landé g factors for electronic spin and nucleus respectively. We have the magnetic moments defined as $\vec{\mu}_L = -\mu_B g_L \vec{L}$, $\vec{\mu}_S = -\mu_B g_S \vec{S}$ and $\vec{\mu}_I = \mu_N g_I \vec{I}$. From the addition of angular momenta which is $\mathbf{J} = \mathbf{L} + \mathbf{S}$ we have the following expression for g_J [13]

$$g_J = g_L \frac{J(J+1) - S(S+1) + L(L+1)}{2J(J+1)} + g_S \frac{J(J+1) + S(S+1) - L(L+1)}{2J(J+1)} \quad (20)$$

For the addition of $\mathbf{F} = \mathbf{J} + \mathbf{I}$ we similarly can write the expression as

$$g_F = g_L \frac{F(F+1) - S(S+1) + L(L+1)}{2F(F+1)} + g_S \frac{F(F+1) + S(S+1) - L(L+1)}{2F(F+1)} \quad (21)$$

In the low field limit we have the Zeeman splitting caused by magnetic field to be much smaller than the hyperfine splitting and so can be written in the following linear form of $H_B = \mu_B g_F \mathbf{F} \cdot \mathbf{B}$. As shown in figure 4, we can see that the splitting constant for a bias field along z axis would be $\Delta = \mu_B g_F m_F \approx 700$ Hz/mG [8]. At higher fields one would have to use the Breit-Rabi formula which has it's second order shown in [11] but will not be of our concern here.

Similar to static fields, oscillating microwave fields (which will be of our main interest here) interact via the following Hamiltonian

$$H_B = \mu_B g_S \mathbf{B} \cdot \mathbf{S} \quad (22)$$

Note that we have ignored the contribution from the nuclear angular momentum since g_I is very small in comparison to g_S . We will be using an oscillatory magnetic field to create Rabi oscillations between the hyperfine levels. For an example we can pick the π transitions which will be referred to as clock transitions. Using RWA the matrix form of the hamiltonian for clock transition levels is written as follow

$$H_0 = \hbar \omega_0 \begin{pmatrix} \frac{3}{8} & 0 \\ 0 & -\frac{5}{8} \end{pmatrix} \quad (23)$$

In the interaction picture the hamiltonian in presence of a magnetic field will be written as follows (here $\Sigma_i = I_{nuc} \otimes \sigma_i$)

$$H_{B,I} = e^{iH_0 t/\hbar} \left(\sum_i B_i(t) \langle F, m_F | \Sigma_i | F', m'_F \rangle \right) e^{-iH_0 t/\hbar} \quad (24)$$

The evolution of state would be given by $i\hbar \dot{\psi} = H_{B,I} \psi$

$$\Omega_{clock} = \frac{\mu_B g_S B_0}{2\hbar} \quad (25)$$

To convert magnetic field to intensity we simply can use the average intensity expression for electromagnetic waves

$$I = \frac{c B_0^2}{2\mu_0} = \frac{c \epsilon_0 E_0^2}{2} \quad (26)$$

For a more general transfer from some state i to f we have the following equation with the matrix element $M_{IF,\{i,f\}}$

$$\Omega_{i,f} = \frac{\mu_B g_S B_0}{2\hbar} M_{IF,\{i,f\}} \quad (27)$$

The transition matrix here from $|F, m_F\rangle$ to $|F', m'_F\rangle$ is defined as $\langle F, m_F | \Sigma_i | F', m'_F \rangle$. We can see that Σ can be written as a rank 1 spherical tensor with components as $\Sigma_0^{(1)} = \Sigma_z$, $\Sigma_{\pm 1}^{(1)} = (\mp \Sigma_x - i \Sigma_y)/\sqrt{2}$. The Wigner-Eckhart theorem states the following

$$\langle F, m_F | \Sigma_q^{(k)} | F', m'_F \rangle = \langle F || T^{(k)} || F' \rangle \langle F', 1; m'_F, q | F, m_F \rangle \quad (28)$$

Where $\langle F', 1; m'_F, q | F, m_F \rangle$ is the Clebsch-Gordan coefficient [10]. From this we get that for the π transition we need linearly polarized light along the z axis (non zero B_z) and for the σ_{\pm} transitions where $m_f = \pm 1$ we need circularly polarized light [8] (RCP for σ_- and LCP for σ_+).

The transition of our interest is going from $|F=1, m_F=1\rangle$ to $|F=2, m_F=2\rangle$ which is a σ_+ transition. The Zeeman effect will be null since the bias field would be set at zero and we only have an oscillatory magnetic field. We get that the desired σ_+ transition has a matrix element that is $\sqrt{3/2}$ times that of the π transition and grouping this along with intensity we get the following relation.

$$\Omega_{|1\rangle \rightarrow |2\rangle} = \frac{e g_S}{4 m_e} \sqrt{\frac{3 \mu_0 I}{c}} = \mathcal{K}_{1,2} \sqrt{I} \quad (29)$$

Taking I to be in W/m² we get $\mathcal{K}_{1,2} \approx 9.866$ kHz·mW^{-0.5}

C. Rabi oscillations in the D_2 line

When describing the Hamiltonian for atom-light interaction, using the RWA we get the following expression for the Rabi frequency

$$\Omega = -\frac{\langle g|\hat{\epsilon} \cdot \mathbf{d}|e\rangle \cdot E_0}{\hbar} \quad (30)$$

As shown in [11], the dipole operator has symmetries which can help us in obtaining photon scattering rates with simpler expressions. The first symmetry tells us that the decay rate Γ is independent of the sublevel chosen for transfer which happens since the matrix elements deciding transfer from any level add up to a constant

$$\sum_{q, F'} |\langle F', m'_F + q | er_q | F', m'_F \rangle|^2 = \frac{2J+1}{2J'+1} |\langle J || er || J' \rangle|^2 \quad (31)$$

If we sum the matrix elements from a single ground state sublevel t the levels in some F' energy level we get the following ($A_q = |\langle F, m_F \rangle \langle F', 1; (m_F - q)q |^2$)

$$\begin{aligned} S_{FF'} &= \sum_q A_q (2F'+1)(2J+1) \left\{ \begin{matrix} J & J' & 1 \\ F' & F & I \end{matrix} \right\}^2 \\ &= (2F'+1)(2J+1) \left\{ \begin{matrix} J & J' & 1 \\ F' & F & I \end{matrix} \right\}^2 \end{aligned} \quad (32)$$

Here $\left\{ \begin{matrix} J & J' & 1 \\ F' & F & I \end{matrix} \right\}$ is the Wigner-6j symbol [14] which is a generalization of Clebsch-Gordan coefficients to function for addition of three angular momenta. We also note that $\sum_{F'} S_{FF'} = 1$ which shows that an isotropic pump field would couple the levels independently from their distributed populations. The factors $S_{FF'}$ decides the relative strength of the different transfers. In case the light is isotropic and couples the two levels, the effective dipole moment is given by

$$|d_{iso,eff}(F \rightarrow F')|^2 = \frac{S_{FF'}}{3} |\langle J || er || J' \rangle|^2 \quad (33)$$

This gives the formula for Rabi frequency as

$$\Omega_{iso} = \sqrt{\frac{S_{FF'}}{3}} |\langle J || er || J' \rangle| \frac{E}{\hbar} \quad (34)$$

Given that intensity is proportional to the square of peak electric field, the rabi frequency will be proportional to \sqrt{I} . The final expression can be written in terms of spontaneous decay rate Γ and I_{sat} which is the saturation intensity. Here $I_{sat} = \frac{c\epsilon_0\Gamma^2\hbar^2}{4|\hat{\epsilon} \cdot \mathbf{d}|^2}$ and $\Gamma = 2\pi \cdot 6.065(9)$ MHz [15]. For the transition that we are interested in which is $|F=2, m_F=2\rangle \rightarrow |F=3, m_F=3\rangle$, we have $I_{sat} = 1.669(2)$ mW/cm² [11].

$$\Omega_{|2\rangle \rightarrow |3\rangle} = \Gamma \sqrt{\frac{I}{2I_{sat}}} = \mathcal{K}_{2,3} \sqrt{I} \quad (35)$$

Taking I to be in W/m², $\mathcal{K}_{2,3} \approx 6.590$ MHz·mW^{-0.5}. Right off the bat comparing this value with $\mathcal{K}_{1,2}$, it is clear that the microwave transition requires a considerably higher amount of intensity to drive it in comparable Rabi frequencies in comparison to the optical transition.

III. STIMULATED RAMAN ADIABATIC PASSAGE

A. Theory

Stimulated Raman Adiabatic Passage (STIRAP) is a process which permits transfer between two states using two coherent electromagnetic pulses. The approach makes use of an intermediate state and the aim is to keep the steady state population of this intermediate state to be very small. For STIRAP [16] we need $\Delta_S = -\Delta_P$ for the two photon resonance in ladder configuration ($E_1 < E_2 < E_3$).

$$\hbar\Delta_P = E_2 - E_1 - \hbar\omega_P \quad (36)$$

$$\hbar\Delta_S = E_3 - E_2 - \hbar\omega_S \quad (37)$$

The effective hamiltonian in the basis of these three states can be written as

$$H = \frac{\hbar}{2} \begin{pmatrix} 0 & \Omega_P(t) & 0 \\ \Omega_P(t) & \Delta & \Omega_S(t) \\ 0 & \Omega_S(t) & \delta \end{pmatrix} \quad (38)$$

We aim to transfer population from $|F=1, m=1\rangle$ to $|F=3, m=3\rangle$ using $|F=2, m=2\rangle$ as an intermediate state. Here we use Ω_P (referred to as arising from the pump laser in common text) for transfer between $|F=1, m=1\rangle$ to $|F=2, m=2\rangle$ which is microwave induced and Ω_S (referred to as arising from the stokes laser in common text) for transfer between $|F=2, m=2\rangle$ to $|F=3, m=3\rangle$ which is done by an optical laser. These have been explained in detail in the previous section.

We define a mixing angle $v(t)$ as $\tan(v(t)) = \Omega_P(t)/\Omega_S(t)$. When there is two photon resonance, one of the eigenvalues of the Hamiltonian is zero. The eigenstate (called as the dark state) for this eigenvalue would be

$$|\phi_0\rangle = \cos(v(t)) |1\rangle - \sin(v(t)) |3\rangle \quad (39)$$

As we can see, there is no population that would go to the intermediate state in such a situation and as long as the mixing angle changes slowly, we would have a successful STIRAP. Populating the second state would come with it's losses due to decay from $|2\rangle$ and so is aimed to be kept low. The other two adiabatic states are as follows [17]

$$|\phi_+\rangle = \sin(v(t)) \sin(\varphi(t)) |1\rangle + \cos(\varphi(t)) |2\rangle + \cos(v(t)) \sin(\varphi(t)) |3\rangle \quad (40)$$

$$|\phi_+\rangle = \sin(v(t)) \sin(\varphi(t)) |1\rangle + \cos(\varphi(t)) |2\rangle + \cos(v(t)) \sin(\varphi(t)) |3\rangle \quad (41)$$

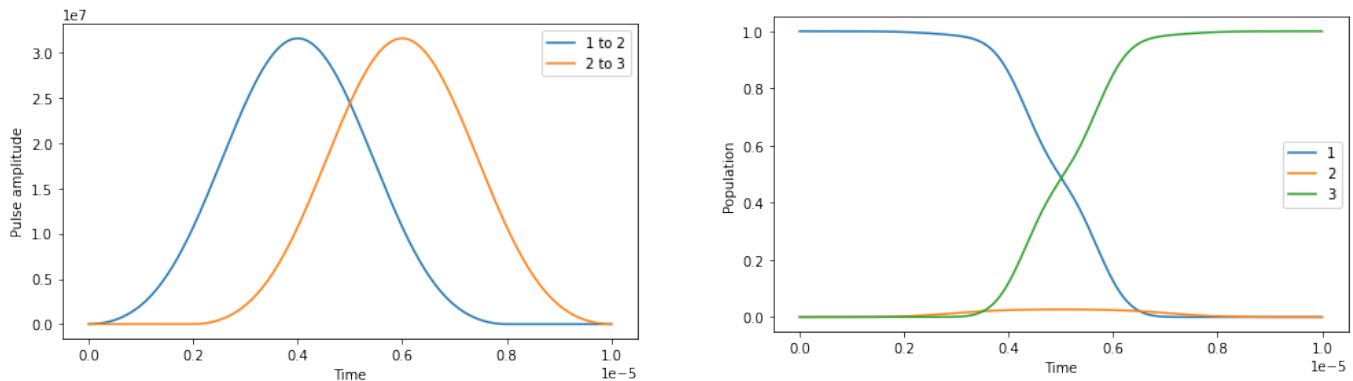


FIG. 5. Simulation results for STIRAP using blackman shaped pulses as shown in the figure on left. Both the pulses have equal Rabi peaks of 31.6 MHz and the timescale of $T = 10\mu\text{s}$ and each pulse is $8\mu\text{s}$ wide. The results (right) show that there is a successful transfer of about 99.9999% efficiency which is pretty much perfect. The $\Delta = 0.1$ GHz and the transfer is particularly *robust*.

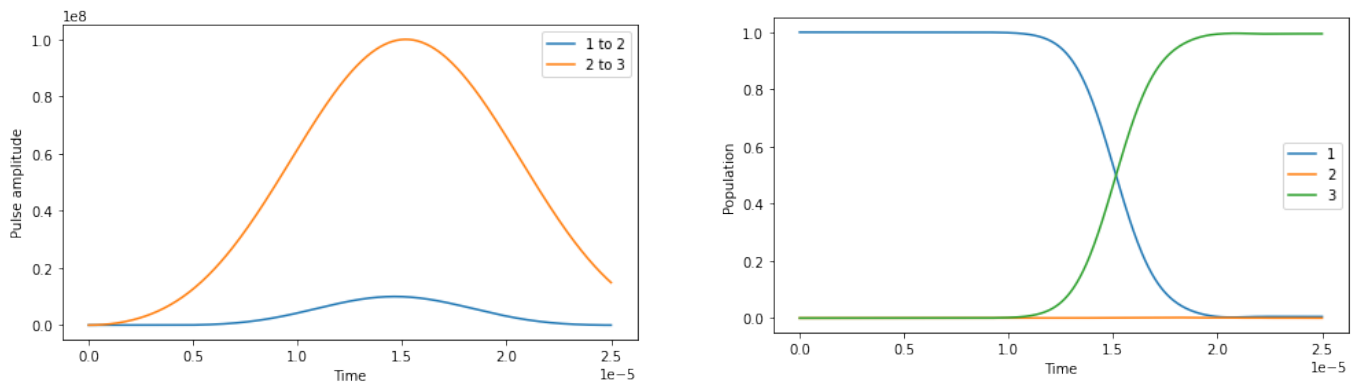


FIG. 6. Simulation results for population transfer using blackman shaped pulses as shown in the figure on left. The pump (1 to 2) pulse had a peak of 10 MHz and the stokes (2 to 3) pulse had a peak of 100 MHz and the timescale $T = 50\mu\text{s}$. Here $\Delta = 1$ GHz and $\delta = 2.182238$ MHz. The aim of this optimization was to see if the transfer can be run efficiently at a smaller timescale and using the scipy optimization we were able to run it at $25\mu\text{s}$ but not any lesser without sacrificing efficiency. The thing to take note of is that the stokes pulse actually ends at beyond the T and while it may seem wrong, this is really the same as multiplying the blackman window which just got cut at the end since the simulation only runs till that point in time after which it is safe to say that both the Rabi frequencies are zero. The stokes pulse would have ended at about $1.20T$ (not considering it being set to zero at T) and the pump pulse begins at $0.163T$. The efficiency achieved was about 99.49% for this parameter set and was also fairly robust to slight variations around these numbers.

Here $\tan(2\varphi(t)) = \frac{\sqrt{\Omega_P(t)^2 + \Omega_S(t)^2}}{\Delta}$. The eigenvalues are $\epsilon_{\pm}(t) = [\Delta \pm \sqrt{\Delta^2 + \Omega_P(t)^2 + \Omega_S(t)^2}]$. If $\Delta = 0$, and at some time both the Rabi frequencies are zero, the three states are degenerate which is lifted off when any of these become non zero referred to as Autler-Townes splitting [18]. The stepwise procedure for STIRAP is as follows [16]

- **Stage 1:** Ω_S is non zero and $\Omega_P = 0$ causing Autler-Townes splitting for $|2\rangle$ and $|3\rangle$. The state vector coincides with the dark state.
- **Stage 2:** Ω_S is much greater than Ω_P which is non zero now. The state deviates slightly from the dark state but the transfer to the two states in equations 24,25 is prevented due to the strong S field causing destructive interference.

- **Stage 3:** Ω_S is in same scale as Ω_P now and the mixing angle increases from 0 to $\pi/2$ and the state remains in the dark state so $|2\rangle$ is left unpopulated.
- **Stage 4:** The state is now nearly aligned to $-|3\rangle$ and Ω_P is much larger than Ω_S and similar to stage 2, this prevents the population in the third state to get transferred elsewhere.
- **Stage 5:** Ω_S is now gone and the P induced Autler-Townes splitting gradually goes to zero and we have the final state as $-|3\rangle$.

Typically one would want the STIRAP to have a very low Δ , $|\Omega_P|, |\Omega_S|$ should be much smaller than the energy differences and we set $\delta = 0$. Under these conditions, it is seen that the results are relatively insensitive

such as pulse shape and timing making the process robust [19]. An important point to note is that under these conditions, the ordering of the pulses must be kept in mind (*SP* order). This is also referred to as counter-intuitive pulse ordering and while the intuitive pulse ordering (*PS*) may work, it is not as robust. Additionally one can include decaying effects by writing the effective detuning as $\Delta' = \Delta - \Gamma/2$ and causes an overall decay in population [20] where Γ is the amount of decay in Hz. Taking $|\psi\rangle = a_1 |F=1, m=1\rangle + a_2 |F=2, m=2\rangle + a_3 |F=3, m=3\rangle$, at large detunings we can take \dot{a}_2 to be close to zero since the oscillations of Δ would average out to zero in the timescale of the pulses [21],[22]. This will reduce the problem to a two dimensional one where the rabi frequency is given by

$$\Omega_{eff}(t) = -\frac{\Omega_P(t)\Omega_S(t)}{\Delta} \quad (42)$$

$$\Delta_{eff}(t) = \frac{\Omega_P(t)^2 - \Omega_S(t)^2}{2\Delta} \quad (43)$$

To get an effective rabi frequency of 1 MHz where the detuning $\Delta = 1$ GHz we can use a microwave rabi frequency peaking at about 10 MHz and an optical rabi frequency peaking at about 100 MHz.

We know that Ω_S is proportional to \sqrt{I} , so for a peak intensity $I = 23.02$ mW/cm², we get the peak $\Omega_S = 100$ MHz based on the value of $\mathcal{K}_{2,3}$. Also we would have $\Omega_{\mu W} = 10$ MHz for magnetic intensity ≈ 1.03 W/mm². As we can see we have no choice but to keep unequal peaks and in the next subsection we discuss why a non zero δ is now very important for this.

B. Importance of two photon detuning

When the Rabi frequencies of the P and S pulses differ significantly, the optimum conditions for population transfer in an ensemble no longer center on two-photon resonance $\delta = 0$ and it may become desirable to select a nonzero value of δ in order for the population transfer to be most effective[19]. That is the reason we get near perfect efficiency irrespective of the value of δ upon plotting efficiency vs δ for equal Rabi frequencies of the P and S pulses. For this, we now study how efficiency changes as we change the two-photon detuning.

C. Robustness of the process

A prominent feature of STIRAP is that it is robust [19, 23]. The robustness specifically refers to a near independence on the parameters of single-photon detunings, pulse shapes, pulse durations, and peak Rabi frequencies or temporal pulse areas. However pulse delays is an important factor which will affect the efficiency.

To properly quantify the resonance, on defining $f =$

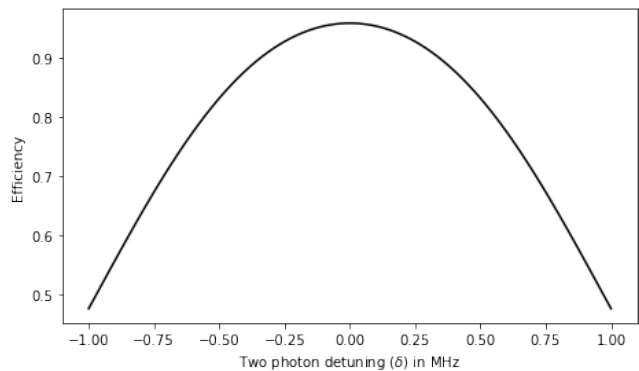


FIG. 7. In the above graph, we have plotted efficiency vs the the two photon detuning, for $T = 0.5$ ms, $\Omega_S = 31.6$ MHz, $\Omega_P = 31.6$ MHz, $\Delta = 0$, $\gamma = 6$ MHz. Here we picked 10 equally spaced points in the range of -1MHz to 1MHz and plotted the efficiency, with the data points connected by a cubic spline for representational purposes.

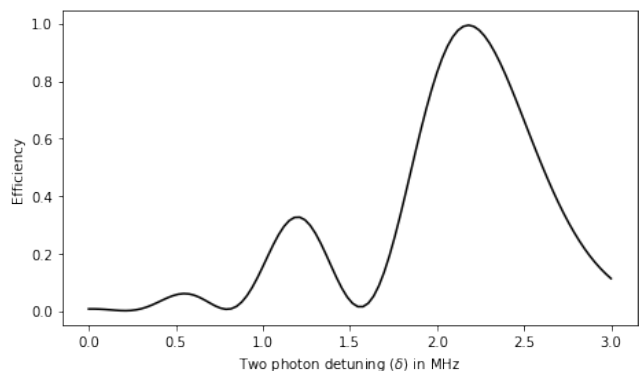


FIG. 8. In the above graph, we have plotted efficiency vs the the two photon detuning, for $T = 0.25$ ms, $\Omega_S = 100$ MHz, $\Omega_P = 10$ MHz, $\Delta = 1$ GHz, $\gamma = 0$. Here we picked 25 equally spaced points in the range of 0 to 3MHz and plotted the efficiency, with the data points connected by a cubic spline for representational purposes.

$|\langle\psi(t)|3\rangle|^2$ which is the actual efficiency, we go on to define a robustness parameter \mathcal{R} as follows

$$\mathcal{R} = \left| \left(\Omega_P \frac{\partial f}{\partial \Omega_P}, \Omega_S \frac{\partial f}{\partial \Omega_S}, \Delta \frac{\partial f}{\partial \Delta}, \delta \frac{\partial f}{\partial \delta}, T \frac{\partial f}{\partial T} \right) \right| \quad (44)$$

This definition is roughly inspired from 5.8c of [19]. One must however note that this does not necessarily accommodate a way to say how pulse shape affects efficiency but will do so for peak values and detunings. A value of \mathcal{R} lesser than 0.01 turns out to be very robust an example of which can be found in figure III A which has $\mathcal{R} \approx 0.0009$.

While one could call that example a success, what we see in figure III A is not very robust as it has a $\mathcal{R} \approx 0.31$. An argument of why this must happen is quite possibly from the sensitivity of the two photon detuning which arises due to an unbalanced Autler-Townes shift when

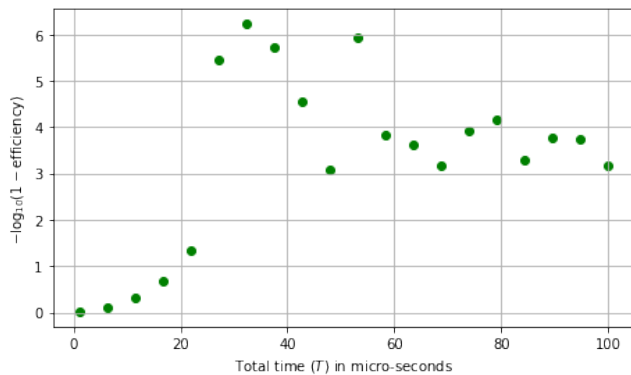


FIG. 9. For the above graph we picked 20 equally spaced points in the range of $1\mu\text{s}$ to $100\mu\text{s}$ and taking each as a value for the total time T we separately optimized their efficiency. The results show that the best possible efficiency for the STIRAP which follows our constraints clearly gets closer to 1 as the T increases and then remains close to a good degree. There is however peculiar behavior particularly once we cross $30\mu\text{s}$ where the efficiency is somewhat oscillating. One can see that this oscillatory nature is expected in the standard STIRAP too [19] making larger times not necessarily always better.

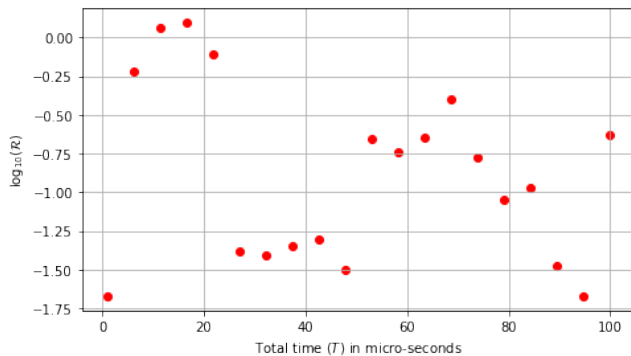


FIG. 10. Shown above is the variation of the robustness factor \mathcal{R} we defined. These robustness were calculated for the same parameters which generated the efficiencies in figure 9. The first four points really tell us nothing as they represent robustness of an inefficient setup, however there is interesting variation even once it does get efficient. In a rough manner, for larger times, there is more robustness however there is not enough points to make a claim about the exact dependence on time. Oddly however while certain points are more robust than others, these only give an idea of the robustness in a small error range and not much for larger ranges hence not necessarily conclusive.

the peaks are unequal.

However based on the contour plot obtained, it points that this might quite possibly be somewhat of a π pulse transfer due to the extremal conditions that have been set on it. Regardless it remains as an example for coherent population transfer albeit not strictly STIRAP.

One must however not be easily swayed by very small \mathcal{R} values as they do not necessarily give very high robust-

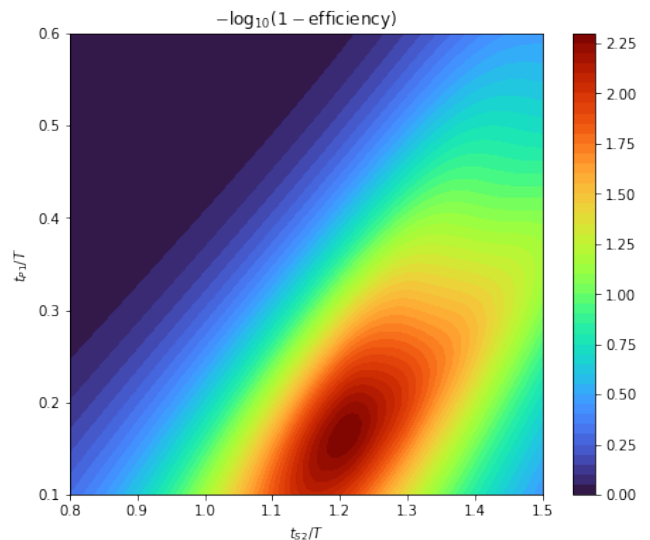


FIG. 11. Shown above is the variation of efficiency for the stirap based on two parameters t_{P1} which is the start of pump pulse and t_{S2} which is the end of the stokes pulse. The total time $T = 25\mu\text{s}$ here and the $\delta = 2.182238$ MHz. As we can see the contour plot which shows the value of efficiency seems to have a well defined maximum over this range. We can visually see that near the maximum which was approached by our previous optimization, there are many points which still boast a very close value of efficiency showing that the choice of parameters does have some breathing space which is a good sign.

ness for large error ranges as we tested with the example of $T = 32\mu\text{s}$ optimized. While having $\mathcal{R} \approx 0.038$, it performed not all too great at even 5% errors. While this may be a bit too much to ask, the equal peak case showed far more promise with being able to withstand 10% errors to a very good degree too.

D. N -STIRAP

We can generalize state transfers to complete population transfer from some $|1\rangle$ to $|N\rangle$ using $|2\rangle \dots |N-1\rangle$ as intermediate states. The number of pulses to use would essentially be $N-1$ and the hamiltonian would be of a tri-diagonal form. The form of the Hamiltonian is the following

$$H = \begin{pmatrix} 0 & \Omega_{1,2}(t) & \dots & 0 \\ \Omega_{1,2}(t) & 2\Delta_2 & \Omega_{2,3}(t) & 0 \\ 0 & \Omega_{2,3}(t) & \ddots & 0 \\ 0 & \dots & \Omega_{N-1,N}(t) & 2\Delta_N \end{pmatrix} \quad (45)$$

Here $\Omega_{i,j}(t)$ is the rabi pulse for transfer between $|i\rangle$ and $|j\rangle$. Each value Δ_i is the effective detuning of $|i\rangle$ from $|1\rangle$ caused by choosing appropriate frequencies for each rabi pulse which can easily be evaluated according to the chosen Δ_i .

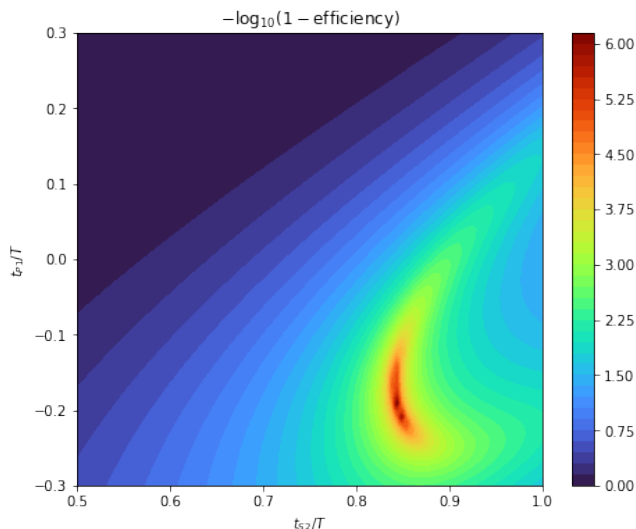


FIG. 12. Shown above is the variation of efficiency for the stirap based on two parameters t_{P1} which is the start of pump pulse and t_{S2} which is the end of the stokes pulse. The total time $T = 32\mu\text{s}$ here and the $\delta = 2.109043$ MHz. In contrast to the analysis for the similar setup for the $T = 25\mu\text{s}$ case, the space of good solutions seems to be fewer and there is clearly two maximas with one being a better maximum. The achieved maximum is better and the system hints at a very nice robustness with $\mathcal{R} \approx 0.038$ at the optimal point.

There are various cases to analyze here which is analyzed in detail in [19, 23]. We demonstrate a simple and efficient toy example of a 4-level state transfer in figure III D. We also developed a framework which is capable of simulating any given N -STIRAP and also optimize it's pulse widths and N -photon detuning.

E. Cavity STIRAP

The potential of STIRAP in cavity Quantum Electrodynamics was realized, instead of just using STIRAP for laser-driven atoms and molecules. It was recognized that STIRAP could be used for creating a well defined photon number (Fock) state of the cavity mode. Parkins et al. [24] proposed to create coherent superpositions of Fock states by mapping a coherent superposition of Zeeman atomic sublevels to the cavity field.

In cavity-STIRAP (or vacuum-STIRAP), a laser beam excites one branch of the Raman transition (usually P) of a single atom, while the cavity vacuum stimulates the emission of the photon on the other branch (usually S). The quantized field of the single-mode cavity provides the Stokes coupling (a vacuum Rabi frequency) denoted by $g(t)\sqrt{n+1}$, where n is the number of photons in the cavity mode and $g(t)$ is the coupling strength in a vacuum, $n = 0$.

Because the Stokes cavity field is quantized, with photon number eigenstates $|n\rangle$, the dynamics is described

by the combined atom-photon states $|\psi, n\rangle = |\psi\rangle |n\rangle$. With the RWA, only three such atom-field states are coupled: $|\psi_1, n\rangle$, $|\psi_2, n\rangle$ $|\psi_3, n+1\rangle$. The dark atom-field state corresponds to energy $E_n = \hbar n\omega$, with ω being the frequency of the cavity mode, and we have

$$|E_n\rangle = \frac{2g(t)\sqrt{n+1}ket\psi_1, n - \Omega_P(t)|\psi_3, n+1\rangle}{\sqrt{4(n+1)g(t)^2 + \Omega_P(t)^2}}$$

The atoms pass through the cavity and interact first with the Stokes cavity field and then with the pump laser field. In the adiabatic limit, complete decoherence-free transfer $|\psi_1, n\rangle \rightarrow |\psi_3, n+1\rangle$ is achieved, without populating the decaying excited state $ket\psi_2, n$. Because of the quantized cavity field, the usual adiabatic condition becomes, for the pump field, $\Omega_P T_P \gg 1$; for the Stokes field, it is $2g_{max}T(n+1) \gg 1$. For an initially empty cavity ($n = 0$), a single-photon state is created out of the vacuum after the atom passes through the cavity. If the atom arrives in a coherent superposition of Zeeman sublevels, then cavity-STIRAP may produce a coherent superposition of Fock states. The transfer of coherence from an atom to a field mode is reversible; likewise, it allows the mapping of cavity fields onto atomic ground-state coherence, which has been suggested as a method for measuring cavity fields.[25]

F. Simulations

QuTip [6, 7] was used for the simulations along with Krotov [27] to both solve the equations of the time dependent Hamiltonian and change pulse shapes for optimized results. The Krotov optimization procedure used is based on an example in the documentation of the package [28]. It must be noted however that the final optimization procedure used was Powell's method [29] with help of the SciPy package. The variables which were used in the optimization were the end time of the stokes pulse, the start time of the pump pulse and the two photon detuning. The start time of stokes was trivially set to 0 and the end time of the pump was also trivially set to T . The final results are demonstrated in figures III A and III A. An important requirement for a successful STIRAP transfer is that $\sqrt{\Omega_P^2 + \Omega_S^2}T \gg 10$ which is a limit obtained by simulations shown in [30]. As shown in figure III A we successfully did manage to get the simulation done for $25\mu\text{s}$ however for smaller times the optimal efficiency did not reach the desired values (see figure 9).

The generalization to N -STIRAP simply made use of Powell's method again this time on start time of the Blackman pulses and their respective widths. It must be noted that while optimization gives a satisfactory value of the efficiency in most cases, the robustness is something which seems to be harder to achieve better values in. As we can see in figure 10 robustness seems to be somewhat hit or miss after a certain time for the chosen example which was analyzed however came quite easily for equal

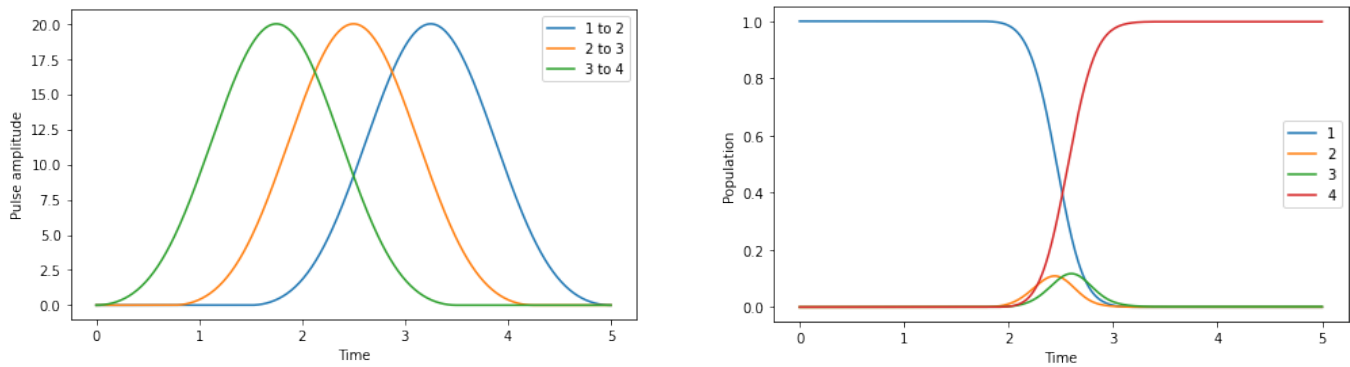


FIG. 13. Simulation results for population transfer using blackman shaped pulses as shown in the figure on left. All the transfers were on resonance and an efficiency of 99.83% was achieved.

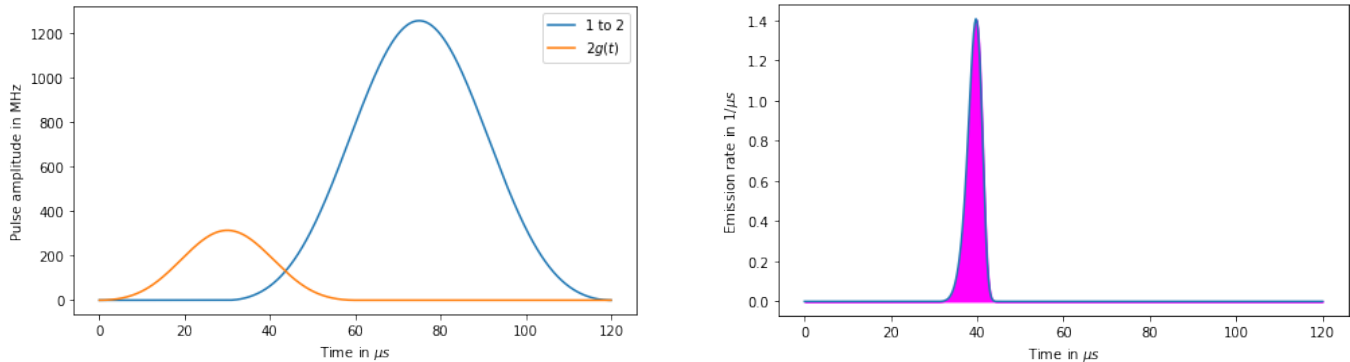


FIG. 14. Simulation results for getting photon emission rate. The cavity coupling is represented by $2g(t)$ and the pump transfer is simply $\Omega_{1 \rightarrow 2}$. The emission rate is defined as $2\kappa |\langle 3|\psi \rangle|^2$ where $\kappa = 2\pi \times 2.5$ MHz is the decay rate of the cavity. The decay rate of the intermediate state is chosen as $\Gamma = 2\pi \times 6$ MHz. The parameters were chosen in reference to [26] to verify the simulation process.

peaks. A better robustness however did not mean much however if the actual robustness is only for small error bounds hence while we can see how in figure ?? we have better efficiency and better robustness for $32\mu s$, it is not any better than $25\mu s$ when we make error ranges of 5% or above.

IV. CONCLUSION AND DISCUSSION

We have in our simulations demonstrated the successful transfer of population between $|F = 1, m_F = 1\rangle$ to $|F = 3, m_F = 3\rangle$ in the large detuning regime. A thing to note is that we have stuck to the Blackman pulse shapes throughout and while these are similar to the Gaussian (upto the sixth central moment) and very practical, one can choose more varying pulse shapes. There is infact a more optimized shape presented in [31] where Dykhne-Davis-Pechukas (DDP) method is used to minimize nonadiabatic transitions and to maximize the fidelity of the resulting STIRAP. Also when using the Krotov method to optimize pulse shapes one would often end up on a pulse which has a shape with varying phase

along with varying amplitude. This however can result in significant levels of population entering the second state which combined with decay can be detrimental. On an additional note we have not used the decay factor of Γ anywhere in our simulations since even if included we would use it to be about 6 MHz based on data discussed in previous sections and so does not actually affect our calculations much.

The cavity-STIRAP simply has the final transfer paired with a photon system and the emission rate is taken as rate of change of probability of emmission of the photon in the cavity. The $2g(t)$ is simply treated as the $\Omega_{N-1,N}(t)$ but the Hamiltonian terms include the paired photon's creation and destruction operators as shown in the cavity STIRAP section.

ACKNOWLEDGEMENTS

We would like to thank Professor Barak Dayan for his guidance since the commencement of this project and for his support and assistance to both of us. We would also like to thank Dr. Jeremy Raskop for analyzing our

simulations and helping understand the subjects at hand better. We have learnt a lot from Professor Dayan and Dr. Raskop over the course of the project and as a result have gained valuable insight into the interesting field of quantum optics. We are very grateful to have received this opportunity and to have spent our summer working

on this project.

CODE AVAILABILITY

All the codes which were used for generating data and the plots for this report can be found at <https://github.com/mahadevans2432/Quantum-Optics>

-
- [1] E. Jaynes and F. Cummings, Comparison of quantum and semiclassical radiation theories with application to the beam maser, *Proceedings of the IEEE* **51**, 89 (1963).
- [2] I. I. Rabi, Space quantization in a gyrating magnetic field, *Phys. Rev.* **51**, 652 (1937).
- [3] J. H. Eberly, N. B. Narozhny, and J. J. Sanchez-Mondragon, Periodic spontaneous collapse and revival in a simple quantum model, *Phys. Rev. Lett.* **44**, 1323 (1980).
- [4] F. D. Bonani, The jaynes-cummings model (2020).
- [5] M. A. Nielsen and I. L. Chuang, *Quantum Computation and Quantum Information: 10th Anniversary Edition*, 10th ed. (Cambridge University Press, USA, 2011).
- [6] J. Johansson, P. Nation, and F. Nori, Qutip: An open-source python framework for the dynamics of open quantum systems, *Computer Physics Communications* **183**, 1760–1772 (2012).
- [7] J. Johansson, P. Nation, and F. Nori, Qutip 2: A python framework for the dynamics of open quantum systems, *Computer Physics Communications* **184**, 1234–1240 (2013).
- [8] P. Joslin, All-microwave control of hyperfine states in ultracold spin-1 rubidium (2019).
- [9] N. C. for Biotechnology Information, Pubchem compound summary for cid 6335802, rubidium-87, online, Accessed June 15, 2021.
- [10] J. J. Sakurai, *Modern quantum mechanics*, rev. ed ed. (Addison-Wesley Pub. Co, 1994).
- [11] D. A. Steck, Rubidium 87 d line data (2019).
- [12] S. Bize, Y. Sortais, M. Santos, C. Mandache Tomescu, A. Clairon, and C. Salomon, High-accuracy measurement of the 87rb ground-state hyperfine splitting in an atomic fountain, *EPL (Europhysics Letters)* **45**, 558 (2007).
- [13] E. E. S. Hans A. Bethe, *Quantum mechanics of one-and two-electron atoms*, 1st ed. (Plenum Pub. Corp, 1977).
- [14] E. W. Weisstein, Wigner 6j-symbol. from mathworld—a wolfram web resource, online, Accessed June 18, 2021.
- [15] U. Volz and H. Schmoranzner, Precision lifetime measurements on alkali atoms and on helium by beam-gas-laser spectroscopy, *Physica Scripta Volume T* **65**, 48 (1996).
- [16] N. Sangouard, L. Yatsenko, B. Shore, and T. Halfmann, Preparation of nondegenerate coherent superpositions in a three-state ladder system assisted by stark shifts, *Physical Review A* **73** (2006).
- [17] U. Gaubatz, P. Rudecki, S. Schieman, and K. Bergmann, Population transfer between molecular vibrational levels by stimulated raman scattering with partially overlapping laser fields. a new concept and experimental results, *The Journal of Chemical Physics* **92**, 5363 (1990), <https://doi.org/10.1063/1.458514>.
- [18] S. H. Autler and C. H. Townes, Stark effect in rapidly varying fields, *Phys. Rev.* **100**, 703 (1955).
- [19] B. Shore, Picturing stimulated raman adiabatic passage: A stirap tutorial, *Advances in Optics and Photonics* **9**, 563 (2017).
- [20] N. V. Vitanov and S. Stenholm, Population transfer via a decaying state, *Phys. Rev. A* **56**, 1463 (1997).
- [21] D. J. Tannor, *Introduction to Quantum Mechanics: A Time-Dependent Perspective* (University Science Books, 2006).
- [22] N. V. Vitanov and S. Stenholm, Analytic properties and effective two-level problems in stimulated raman adiabatic passage, *Phys. Rev. A* **55**, 648 (1997).
- [23] N. V. Vitanov, A. A. Rangelov, B. W. Shore, and K. Bergmann, Stimulated raman adiabatic passage in physics, chemistry, and beyond, *Reviews of Modern Physics* **89**, 10.1103/revmodphys.89.015006 (2017).
- [24] A. S. Parkins, P. Marte, P. Zoller, and H. J. Kimble, Synthesis of arbitrary quantum states via adiabatic transfer of zeeman coherence, *Phys. Rev. Lett.* **71**, 10.1103/PhysRevLett.71.3095 (1993).
- [25] A. S. Parkins, P. Marte, P. Zoller, O. Carnal, and H. J. Kimble, Quantum-state mapping between multi-level atoms and cavity light fields, *Phys. Rev. Lett.* **51**, 10.1103/PhysRevA.51.1578 (1995).
- [26] M. Hennrich, T. Legero, A. Kuhn, and G. Rempe, Vacuum-stimulated raman scattering based on adiabatic passage in a high-finesse optical cavity, *Physical Review Letters* **85**, 4872–4875 (2000).
- [27] M. H. Goerz, D. Basilewitsch, F. Gago-Encinas, M. G. Krauss, K. P. Horn, D. M. Reich, and C. P. Koch, Krotov: A Python implementation of Krotov’s method for quantum optimal control, *SciPost Phys.* **7**, 80 (2019).
- [28] M. Goerz, Optimization of a state-to-state transfer in a lambda system in the rwa, online. Accessed June 18th, 2021.
- [29] M. J. D. Powell, An efficient method for finding the minimum of a function of several variables without calculating derivatives, *The Computer Journal* **7**, 155 (1964), <https://academic.oup.com/comjnl/article-pdf/7/2/155/959784/070155.pdf>.
- [30] K. Bergmann, H. Theuer, and B. W. Shore, Coherent population transfer among quantum states of atoms and molecules, *Rev. Mod. Phys.* **70**, 1003 (1998).
- [31] G. S. Vasilev, A. Kuhn, and N. V. Vitanov, Optimum pulse shapes for stimulated raman adiabatic passage, *Phys. Rev. A* **80**, 013417 (2009).